Power-Sharing between Grid-Forming and Grid-Following Inverters

Fahmid Sadeque, *Student Member, IEEE*, Dushyant Sharma, *Member, IEEE* and Behrooz Mirafzal, *Senior Member, IEEE*
Department of Electrical and Computer Engineering, Kansas State University, Manhattan, KS, USA
fahmidsadeque@ksu.edu; dushyants@ksu.edu; mirafzal@ksu.edu

***Abstract*—Power-sharing between the grid-forming and the grid-following inverter in a small microgrid is a challenging task. Specifically, the decentralized droop-based power-sharing is difficult to achieve when the grid-forming inverter regulates the voltage and the frequency. This article proposes controllers for the grid-forming and the grid-following inverters, which ensure proportional power-sharing as well as regulate the voltage and the frequency. Both controllers use active power-frequency and reactive power-voltage droops. Additional secondary loops and secondary forward paths are added to the controller of the grid-forming inverter and the grid-following inverter, respectively, to ensure simultaneous voltage and frequency regulation and power-sharing. The efficacy of the proposed controllers for power-sharing is verified through experiment results in a multi-inverter testbed.**

Keywords—Decentralized power-sharing, droop, grid-following inverters, grid-forming inverters, voltage and frequency control.

I. INTRODUCTION

The next-generation inverters are expected to play major roles in the modern power system. With the increase of the number of distributed generations (DGs), the inverters are being used in grid-interactive operations to provide interfaces to the DGs to penetrate the grid [1]-[3]. Besides, the inverters are also capable of providing different ancillary services, such as maximum utilization of DC bus [4], stability enhancement in the weak grid and in abnormal conditions [5]-[11], and mitigation of the voltage and frequency fluctuation [12], [13].

An inverter can mainly operate in two modes– grid-forming and grid-following. The grid-forming inverters can operate independently by regulating the output voltage of the inverter and the system frequency. This type of inverter is useful for initiating the operation of an islanded microgrid after a black-out, when the main grid is not available. However, they cannot control the active and reactive power injection. The grid-following inverters can supply a specified active and reactive power. However, this type of inverters does not have control on voltage and frequency, and hence are dependent on other generators [14], [15]. As the next generation microgrids are going to be more dependent on the inverters, and all inverter-based nanogrids may emerge [16], the need for controller to ensure the power-sharing between the grid-forming and the grid-following inverters has also emerged.

This work is supported in part by the Department of Energy, Office of Energy Efficiency and Renewable Energy (EERE), Solar Energy Technologies Office, under Award Number DE-EE0008767, and National Science Foundation under Award Number ECCS 1920266.

The existing research on power-sharing between multiple inverters can be classified into three major categories– centralized, decentralized, and distributed control. In centralized control and in distributed control, the inverter control is dependent on a single central server or some distributed servers and communication between the servers is required [17]. The dependency on the central server increases the risk of cyberattack. On the other hand, decentralized control methods do not require any form of communication and hence have no risk of cyberattack. The control methods include different types of droop techniques [18]-[26]. Conventional droop based methods adopt active power-frequency (P-f) droop control and reactive power-voltage (Q-V) droop control for decentralized and autonomous power-sharing [23], [24]. Nevertheless, with conventional droop, the output voltage and the frequency may deviate from the nominal values when the load is not at its nominal value. For an all inverter-based microgrid, the grid-forming inverters can restore the output voltage and the frequency of the system to the desired nominal values. Then, the droop-features of the grid-following inverters will not be useful and the power injections will remain unaffected. As a consequence, any change in the load of a microgrid will only impact the grid-forming inverters. To the best of the authors knowledge, control methods which ensure decentralized power-sharing between the grid-forming and the grid-following inverters as well as regulates the voltage and the frequency of the system are yet to be developed.

This article proposes control methods for power-sharing between the grid-forming and the grid-following inverters in all inverter-based microgrid. The proposed grid-forming inverter controller has active power-frequency and reactive power-voltage droops to enable power sharing. Two secondary loops are added to the controller to restore the voltage and the frequency to their nominal values. Similarly, the two droops are added to the grid-following inverter controller. Two secondary forward paths are added to the droop relationships to enable power-sharing after the voltage and the frequency being restored by the grid-forming inverters. Unlike conventional controllers with droops, the proposed controllers can ensure decentralized power sharing as well as maintain the voltages and frequency of the microgrid to the nominal values. In addition to this introduction, the rest of the article is organized as follows. Section-II briefly describes the system under study. The proposed controllers are presented in section-III. Experimental results are provided in section-IV. Section-V concludes the article by discussing the contribution and the future aspects.

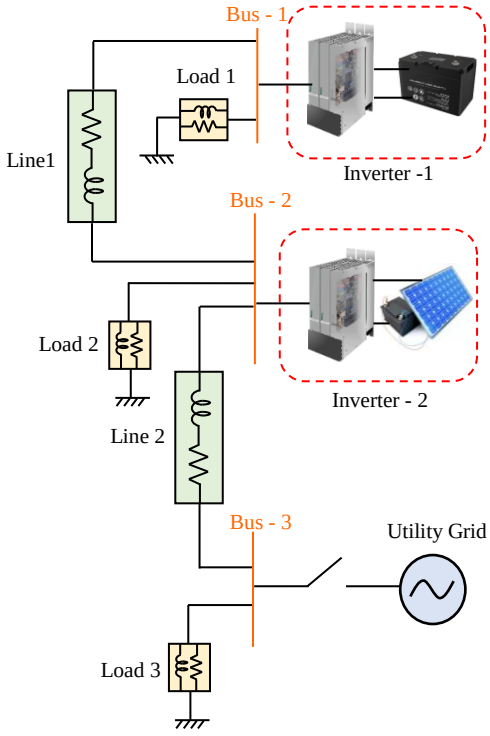

Fig. 1. Schematic diagram of an inverter-based microgrid.

II. System Description

This section provides a brief description of the microgrid considered for this article. The schematic diagram of the system is depicted as in Fig. 1. The microgrid consists of two inverters fed from individual DC sources. Note that, the DC source dynamics are out of the scope of this article, and hence, only constant supplies are considered. Both inverters have measurements sensors for voltage and current measurements. The inverters can operate in both grid-forming mode and grid-following mode. A three-phase load is connected at the point of common coupling (PCC) of inverter-I. The line impedances are represented by a series of resistors and inductors. In this article, inverter-1 at bus-1 is operated as the grid-forming inverter and inverter-2 at bus-2 is operated as the grid-following inverter. Note that, the proposed controller is applicable to any number of inverters in the microgrid.

III. The Proposed Controllers

In this section the proposed controllers for the grid-forming and the grid-following inverters are presented.

A. *Proposed Grid-Forming Inverter Controller.*

Fig. 2 shows the block diagram of the proposed grid-forming inverter controller. The inverter measures the line-line voltages, v_{pcc}, at the PCC and the line-currents, i_L and produces the phase-angle, θ_{inv} and the magnitude of the voltage reference, V_{inv} for the PWM generator of the inverter. Notice, the reference frequency, ω^* and the reference voltage, V^* are predefined in a typical grid-forming inverter, if no droops are required. Hence, the grid-forming inverter can operate independently. To ensure power sharing between multiple inverters, active power-frequency and reactive power-voltage droops is added to the

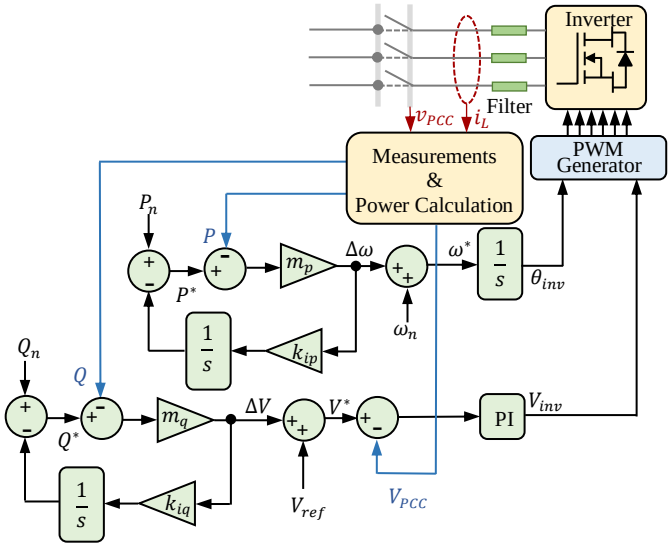

Fig. 2. Block diagram of the proposed grid-forming inverter controller.

inverter controller. In addition, to restore the frequency of the system to the nominal value, ω_n, a secondary-loop is added to the active power droop relationship in the proposed controller. The active power-frequency droop equations with the secondary control loop can be expressed as-

$$\begin{cases} \Delta\omega = m_p(P^* - P) \\ P^* = P_n - K_{ip}\int \Delta\omega dt \end{cases} \quad (1)$$

where, P and P_n are the measured and the nominal reference active power, respectively, and m_p and K_{ip} are the droop coefficient and loop gain coefficient, respectively. The reference frequency, ω^* is obtained by adding $\Delta\omega$ with the nominal reference frequency, ω_n, i.e., $\omega^* = \omega_n + \Delta\omega$.

Similarly, the amplitude of the voltages at the PCC can be restored by using another secondary control loop with the reactive power-voltage droop relationship. The loop equations are-

$$\begin{cases} \Delta V = m_q(Q^* - Q) \\ Q^* = Q_n - K_{iq}\int \Delta V dt \end{cases} \quad (2)$$

where, Q and Q_n are the measured and the nominal reference reactive power, respectively, and m_q and K_{iq} are the droop coefficient and loop gain coefficient, respectively. The reference voltage amplitude, V^* is obtained by adding ΔV with the nominal reference voltage amplitude, V_n, i.e., $V^* = V_n + \Delta V$. Note that, the speed of the secondary control loop must be slower than the grid-forming inverter controller to ensure proper power-sharing between multiple inverters.

B. *Proposed Grid-Following Inverter Controller.*

Fig. 3 shows the block diagram proposed grid-following inverter controller. The operation of the grid-following inverter relies on an already operating system. Hence, the controller measures the bus voltage, v_{bus}, and obtains the frequency, ω^* and the phase-angle, θ_{inv} from its phase-locked loop (PLL). A typical grid-following controller measures the active and

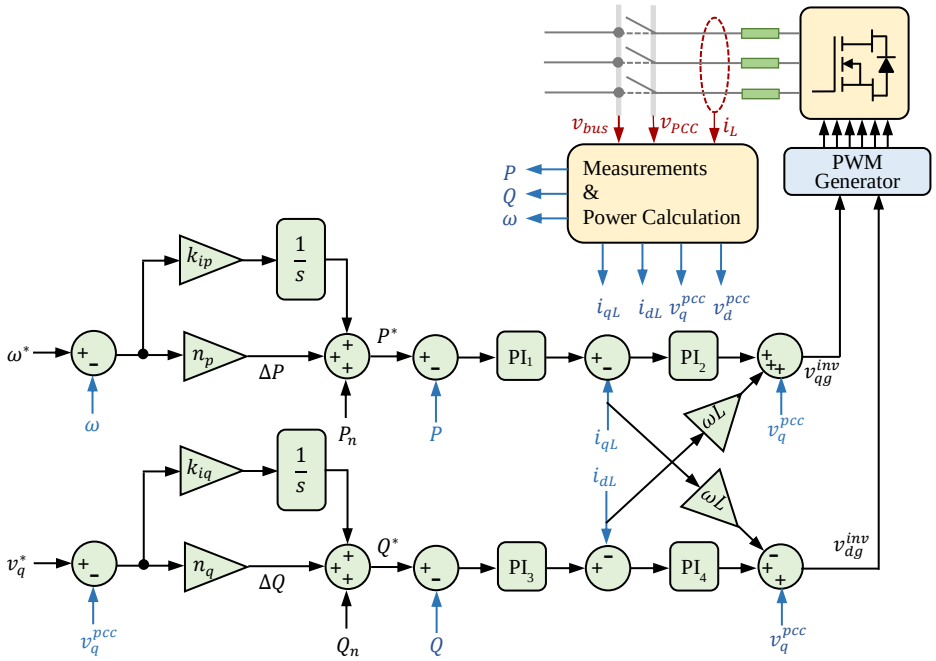

Fig. 3. Block diagram of the proposed grid-following inverter controller.

reactive power injection, P and Q, by the inverter and regulates the power injection to match with the reference active and reactive power values, P^* and Q^*, respectively. Two proportional-integral (PI) loops combined with cross-coupling paths are used in to control each type of power injection. To enable power sharing, active power frequency and reactive power-voltages droops are utilized. Nevertheless, the conventional droop controller cannot perform with the proposed grid-forming inverter controllers. Hence, an integral forward path is added to each of the loops to ensure power sharing while the system frequency and the voltage are restored. The modified active power-frequency droop can be expressed as-

$$P^* = P_n + n_p\Delta\omega + K_{ip}\int \Delta\omega dt \qquad (3)$$

where, $\Delta\omega = \omega^* - \omega$, P^* and P_n are the reference active power and the nominal active power, respectively, and n_p and K_{ip} are the forward path coefficients and the droop coefficients, respectively.

Similarly, the modified reactive power-voltage droop can be expresses as-

$$Q^* = Q_n + n_q\Delta V + K_{iq}\int \Delta v_q dt \qquad (4)$$

where, $\Delta v = v_q^* - v_q^{pcc}$, Q^* and Q_n are the reference reactive power and the nominal reactive power, respectively, and n_q and K_{iq} are the forward path coefficients and the droop coefficients, respectively. The advantage of the additional integral paths is, while the secondary control loops of the grid-forming inverter adjusts the frequency and the voltages, the integral path of the grid-following inverter accounts for the additional change in power to be injected by the grid-following inverters. Hence, decentralized power-sharing and frequency and voltage control, both can be achieved from the proposed controllers.

IV. Experiment Results

This section provides the experimental verifications of the proposed controllers for power-sharing. Fig. 4 shows the

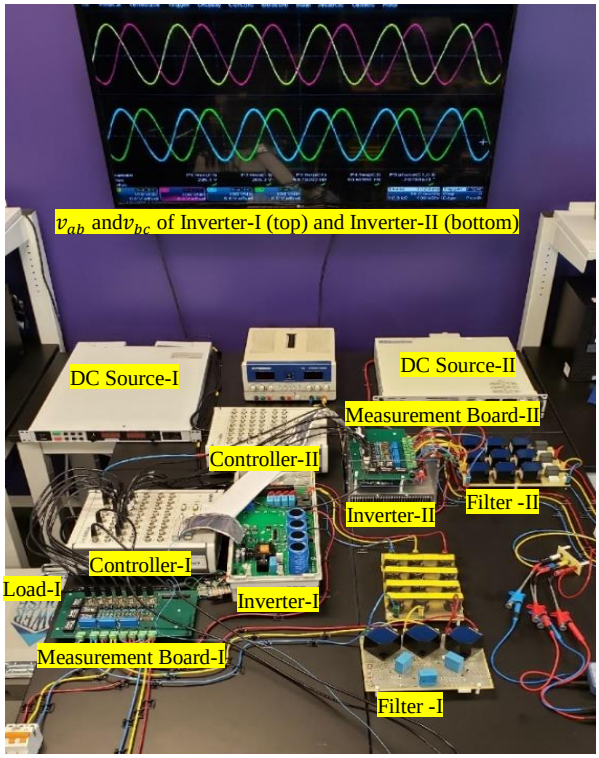

Fig. 4. Experimental setup showing Inverter-I and Inverter-II, operating in grid-forming and grid-following mode, respectively.

TABLE I
IMPORTANT PARAMETERS VALUES FOR EXPERIMENT

Parameters	Values
Nominal Line-Line rms Voltage, V_{LL}	208 V
DC Bus Voltage, V_{DC}	350 V
Nominal Frequency, f	60 Hz
PWM Switching frequency	5 kHz
LCL Filter Inductance (Inverter Side)	1.0 mH
LCL Filter Inductance (PCC Side)	0.5 mH
LCL Filter Capacitance (in Y)	5 μF
Droop Parameters for Inverter-I	
Frequency-active power droop, m_p	0.005
Voltage-reactive power droop, m_q	0.001
Secondary control loop gain-parameters	$k_{ip} = k_{iq} = 0.1$
Droop Parameters for Inverter-II	
Frequency-active power droop, n_p	200
Voltage-reactive power droop, n_q	1000
Secondary forward-path gain-parameters	$k_{ip} = k_{iq} = 10$
Controller Gain Parameters for Inverter-I and II	
Integral and proportional gain for Inverter-I	$k_i = 0.25$, $k_p = 0.0005$
Integral and proportional gain for Inverter-II	$k_i = 0.10$, $k_p = 0.0005$

experimental setup developed for testing the controllers. A small microgrid, consists of two inverters, representing the schematic shown in Fig. 1 was developed. The microgrid consisted of a 10 kVA Allen Bradley Powerflex 755 commercial inverter (Inverter-I) and a 5 kVA laboratory assembled SiC MOSFET-based three-phase inverter (Inverter-II). Two Magna-Power SL400-15/208 programmable DC sources provided the Dc supplies to the inverters. Two dSPACE MicroLabBox DS-1202 digital signal processors (DSPs) were used as controllers and were operated through ControlDesk software. The measurements were obtained through two high-precision measurement boards. Teledyne LeCroy oscilloscopes were used to observe the voltages and currents of the system. All the experiment data were obtained from the ControlDesk software and plotted using MATLAB. Inverter-I was operated as the grid-forming inverter, and inverter-II was operated as the grid-following inverter. Important circuit and controller parameters are provided in Table I. The following cases were investigated.

Case I: Performance of The Grid-Forming Inverter Controller under Load Variation

This test was performed to verify the effectiveness of the grid-forming inverter controller in frequency restoration under load variation. Here, the grid-forming inverter (inverter-I) was operating at 60 Hz, 208 V. A three-phase resistive load of 250 W was connected to the system. The load was increased to 740 W at the 18 s. Fig. 5 shows the experiment result of the aforementioned test. As shown in Fig. 5, the frequency of the system first dropped to 59.61 Hz from 60 Hz due to the increase in the active power injection by inverter-I. This happened due to the droop relationship, that instantaneously changed the frequency reference. The secondary control loop gradually increased the frequency to 60 Hz within the 60^{th} s.

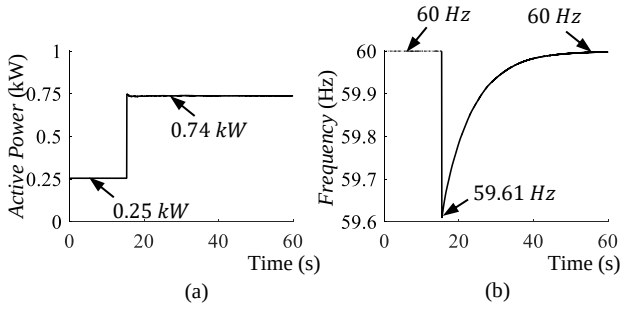

Fig. 5. Experimental result showing the performance of the proposed grid-forming inverter controller during load variation. (a) Active power injected by inverter-I. (b) Frequency of the system.

Here, the speed of the secondary controller was intentionally made slow to show the impact properly. The speed could be made faster by setting higher values of gain. Nevertheless, the speed must be slower than the speed of the inverter controller loop to ensure proper power sharing.

Case II:Power-Sharing between The Grid-Forming and The Grid-Following Inverter Controllers.

In this scenario, the proposed controllers for the grid-forming inverter and the grid-following inverter were tested together to obtain power sharing. To initiate the testing, the grid-following inverter was activated at first to build up the system voltage and provide a frequency and phase-angle reference to the system. Here, a 480 W of load was connected to the system. The grid-following inverter was connected to the system after matching the voltage and the phase-angle with the same parameters at the PCC. Fig. 6 shows the experiment results after

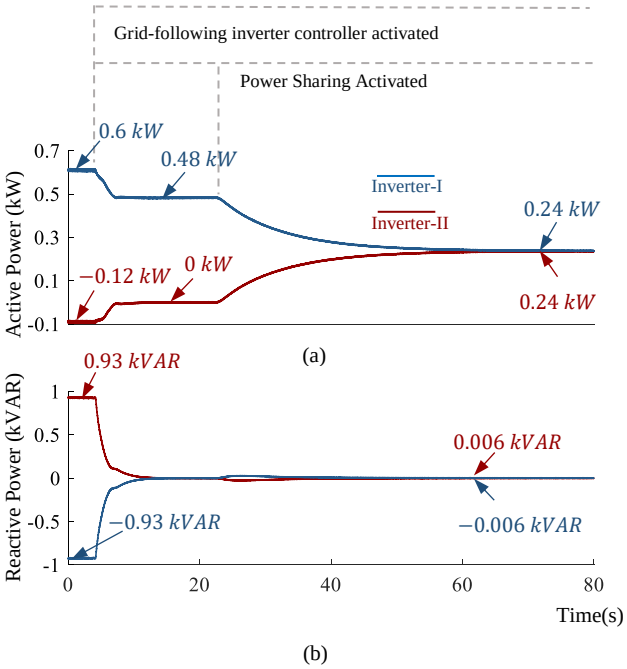

Fig. 6. Experimental result showing the performance of the proposed grid-forming and grid-following inverter controller in equal power sharing. (a) Active power injection of the two inverters, and (b) reactive power injection of the two inverters.

the grid-following inverter was connected. Notice, the grid-following inverter was absorbing active power until the power-control loops of the grid-following inverters were activated at $5\ s$. Then, the grid-following inverter was just connected to the system but not injecting any power. The proposed power-sharing method was activated at $24\ s$. As seen in Figs. 6(a) and 6(b), the two inverters gradually share the total load connected. Note that, for grid-following inverter, the secondary forward loops must not be faster than the secondary controller loop of the grid-forming inverter. Otherwise, power sharing might not be achieved properly.

V. Conclusion

This article has presented a grid-forming and a grid-following inverter controller for power-sharing between the inverters. The grid-forming inverter has droop-based decentralized control with two secondary control loops proposed to restore the frequency and the voltage. Two secondary forward path has been added to the grid-following inverter controller to ensure that the active and reactive power injection is affected when there is change in the load. The efficacy of the developed controllers have been verified through the experiment results. A combined operation of the two methods has provided a solution to the trade-off between proper power sharing, and voltage and frequency regulation between the grid-forming and grid-following inverters. This work can guide the future research on the application of power-sharing in symmetrical and asymmetrical grid in the field of all-inverter based smart power-grid.

References

[1] B. Mirafzal and A. Adib, “On grid-interactive smart inverters: features and advancements,” *IEEE Access*, vol. 8, pp. 160526-160536, 2020.

[2] Y. Niazi, M. E. H. Golshan and H. H. Alhelou, "Combined firm and renewable distributed generation and reactive power planning," *IEEE Access*, vol. 9, pp. 133735-133745, 2021.

[3] D. Sharma and S. Mishra, "Disturbance-observer-based frequency regulation scheme for low-inertia microgrid systems," *IEEE Syst. J.*, vol. 14, no. 1, pp. 782-792, March 2020.

[4] A. Adib, J. Lamb and B. Mirafzal, “Ancillary services via VSIs in microgrids with maximum DC-bus voltage utilization,” *IEEE Trans. Ind. Appl.*, vol. 55, no. 1, pp. 648-658, Jan.-Feb. 2019.

[5] Á. Borrell, M. Velasco, J. Miret, A. Camacho, P. Martí and M. Castilla, “Collaborative voltage unbalance elimination in grid-connected AC microgrids with grid-feeding inverters,” *IEEE Trans. Power Electron.*, vol. 36, no. 6, pp. 7189-7201, June 2021

[6] A. Adib, F. Fateh and B. Mirafzal, "Smart inverter stability enhancement in weak grids using adaptive virtual-inductance," *IEEE Trans. Ind. Appl.*, vol. 57, no. 1, pp. 814-823, Jan.-Feb. 2021.

[7] F. Sadeque and B. Mirafzal, "Cooperative inverters to overcome PLL malfunctions," *in Proc.* 2021 IEEE 12th International Symposium on Power Electronics for Distributed Generation Systems (PEDG), 2021, pp. 1-6.

[8] F. Nejabatkhah, Y. W. Li and B. Wu, "Control strategies of three-phase distributed generation inverters for grid unbalanced voltage compensation," *IEEE Trans. Power Electron.*, vol. 31, no. 7, pp. 5228-5241, July 2016.

[9] A. Adib, B. Mirafzal, X. Wang and F. Blaabjerg, "On stability of voltage source inverters in weak grids," *IEEE Access*, vol. 6, pp. 4427-4439, 2018.

[10] F. Sadeque, J. Benzaquen, A. Adib and B. Mirafzal, “Direct phase-angle detection for three-phase inverters in asymmetrical power grids,” *IEEE J. Emerg. Sel. Topics Power Electron.*, vol. 9, no. 1, pp. 520-528, Feb. 2021.

[11] T. Hossen, F. Sadeque, M. Gursoy and B. Mirafzal, "Self-secure inverters against malicious setpoints," *in Proc.* 2020 IEEE Electric Power and Energy Conference (EPEC), 2020, pp. 1-6.

[12] X. Chen, Y. Hou, S. Tan, C. Lee and S. Y. R. Hui, "Mitigating voltage and frequency fluctuation in microgrids using electric springs," *IEEE Trans. Smart Grid*, vol. 6, no. 2, pp. 508-515, March 2015.

[13] M. S. Pilehvar and B. Mirafzal, "PV-fed smart inverters for mitigation of voltage and frequency fluctuations in islanded microgrids," *in Proc.* 2020 International Conference on Smart Grids and Energy Systems (SGES), 2020, pp. 807-812.

[14] X. Huang, K. Wang, J. Qiu, L. Hang, G. Li, and X. Wang, "Decentralized control of multi-parallel grid-forming DGs in islanded microgrids for enhanced transient performance," *IEEE Access*, vol. 7, pp. 17958-17968, 2019.

[15] H. Han, X. Hou, J. Yang, J. Wu, M. Su, and J. M. Guerrero, "Review of power sharing control strategies for islanding operation of AC microgrids," *IEEE Trans. Smart Grid*, vol. 7, no. 1, pp. 200-215, Jan. 2016.

[16] M. S. Pilehvar, M. B. Shadmand and B. Mirafzal, “Analysis of smart loads in nanogrids,” IEEE Access, vol. 7, pp. 548-562, 2019.

[17] M. Ramezani, S. Li, and Y. Sun, "Combining droop and direct current vector control for control of parallel inverters in microgrid," *IET Renewable Power Generation*, vol. 11, no. 1, pp. 107-114, Nov. 2017.

[18] Y. Chen, J. M. Guerrero, Z. Shuai, Z. Chen, L. Zhou, and A. Luo, "Fast reactive power sharing, circulating current and resonance suppression for parallel inverters using resistive-capacitive output impedance," *IEEE Trans. Power Electron.*, vol. 31, no. 8, pp. 5524-5537, Aug. 2016.

[19] Q. Zhong and G. Weiss, "Synchronverters: inverters that mimic synchronous generators," *IEEE Trans. Ind. Electron.*, vol. 58, no. 4, pp. 1259-1267, April 2011.

[20] T. Wu, Z. Liu, J. Liu, S. Wang, and Z. You, "A unified virtual power decoupling method for droop-controlled parallel inverters in microgrids," *IEEE Trans. Power Electron.*, vol. 31, no. 8, pp. 5587-5603, Aug. 2016.

[21] A. Milczarek, M. Malinowski, and J. M. Guerrero, "Reactive power management in islanded microgrid—proportional power sharing in hierarchical droop control," *IEEE Trans. Smart Grid*, vol. 6, no. 4, pp. 1631-1638, July 2015.

[22] J. M. Guerrero, Luis Garcia de Vicuna, J. Matas, M. Castilla, and J. Miret, "Output impedance design of parallel-connected UPS inverters with wireless load-sharing control," *IEEE Trans. Ind. Electrons.*, vol. 52, no. 4, pp. 1126-1135, Aug. 2005.

[23] J. M. Guerrero, J. Matas, L. Garcia de Vicuna, M. Castilla, and J. Miret, "Decentralized control for parallel operation of distributed generation inverters using resistive output impedance," *IEEE Trans. Ind. Electrons*, vol. 54, no. 2, pp. 994-1004, April 2007.

[24] Y. A. I. Mohamed and E. F. El-Saadany, "Adaptive decentralized droop controller to preserve power sharing stability of paralleled inverters in distributed generation microgrids," *IEEE Trans. Power Electrons.*, vol. 23, no. 6, pp. 2806-2816, Nov. 2008.

[25] Q. Zhong, "Robust droop controller for accurate proportional load sharing among inverters operated in parallel," *IEEE Trans. Ind. Electrons.*, vol. 60, no. 4, pp. 1281-1290, April 2013.

[26] A. Firdaus, D. Sharma, and S. Mishra, " Dynamic power flow based simplified transfer function model to study instability of low-frequency modes in inverter-based microgrids," *IET Generation, Transmission, and Distribution*, vol. 14, no. 23, pp. 5634-5645, Dec. 2020.